



Swansea University
Prifysgol Abertawe



Cronfa - Swansea University Open Access Repository

This is an author produced version of a paper published in :

Journal of Bacteriology

Cronfa URL for this paper:

<http://cronfa.swan.ac.uk/Record/cronfa31099>

Paper:

Fuchino, K., Flårdh, K., Dyson, P. & Ausmees, N. (2016). Cell-biological studies of osmotic shock response in *Streptomyces* spp.. *Journal of Bacteriology*, 199(1), JB.00465-16

<http://dx.doi.org/10.1128/JB.00465-16>

This article is brought to you by Swansea University. Any person downloading material is agreeing to abide by the terms of the repository licence. Authors are personally responsible for adhering to publisher restrictions or conditions. When uploading content they are required to comply with their publisher agreement and the SHERPA RoMEO database to judge whether or not it is copyright safe to add this version of the paper to this repository.

<http://www.swansea.ac.uk/iss/researchsupport/cronfa-support/>



Cell-Biological Studies of Osmotic Shock Response in *Streptomyces* spp.

Katsuya Fuchino,^a Klas Flårdh,^a Paul Dyson,^b Nora Ausmees^{a†}

Department of Biology, Lund University, Lund, Sweden^a; Swansea University Medical School, Swansea, United Kingdom^b

ABSTRACT Most bacteria are likely to face osmotic challenges, but there is yet much to learn about how such environmental changes affect the architecture of bacterial cells. Here, we report a cell-biological study in model organisms of the genus *Streptomyces*, which are actinobacteria that grow in a highly polarized fashion to form branching hyphae. The characteristic apical growth of *Streptomyces* hyphae is orchestrated by protein assemblies, called polarisomes, which contain coiled-coil proteins DivIVA and Scy, and recruit cell wall synthesis complexes and the stress-bearing cytoskeleton of FilP to the tip regions of the hyphae. We monitored cell growth and cell-architectural changes by time-lapse microscopy in osmotic upshift experiments. Hyperosmotic shock caused arrest of growth, loss of turgor, and hypercondensation of chromosomes. The recovery period was protracted, presumably due to the dehydrated state of the cytoplasm, before hyphae could restore their turgor and start to grow again. In most hyphae, this regrowth did not take place at the original hyphal tips. Instead, cell polarity was reprogrammed, and polarisomes were redistributed to new sites, leading to the emergence of multiple lateral branches from which growth occurred. Factors known to regulate the branching pattern of *Streptomyces* hyphae, such as the serine/threonine kinase AfsK and Scy, were not involved in reprogramming of cell polarity, indicating that different mechanisms may act under different environmental conditions to control hyphal branching. Our observations of hyphal morphology during the stress response indicate that turgor and sufficient hydration of cytoplasm are required for *Streptomyces* tip growth.

IMPORTANCE Polar growth is an intricate manner of growth for accomplishing a complicated morphology, employed by a wide range of organisms across the kingdoms of life. The tip extension of *Streptomyces* hyphae is one of the most pronounced examples of polar growth among bacteria. The expansion of the cell wall by tip extension is thought to be facilitated by the turgor pressure, but it was unknown how external osmotic change influences *Streptomyces* tip growth. We report here that severe hyperosmotic stress causes cessation of growth, followed by reprogramming of cell polarity and rearrangement of growth zones to promote lateral hyphal branching. This phenomenon may represent a strategy of hyphal organisms to avoid osmotic stress encountered by the growing hyphal tip.

KEYWORDS *Streptomyces*, apical growth, bacterial cytoskeleton, osmotic stress response, turgor

Environmental bacteria need to cope with sudden changes of extracellular osmotic pressure. They have therefore evolved mechanisms that enable them to adjust their internal conditions, with the ultimate goal of maintaining or resuming growth accordingly. The main consequence of hypo- or hyperosmotic stress is altered water flow into or out of the cells, respectively, meaning that the hydration status of the cells can change drastically within seconds (1). Hypo-osmotic stress can be met directly by the activation of mechanosensitive ion channels to avoid the increase in turgor pressure

Received 20 June 2016 Accepted 5 October 2016

Accepted manuscript posted online 17 October 2016

Citation Fuchino K, Flårdh K, Dyson P, Ausmees N. 2017. Cell-biological studies of osmotic shock response in *Streptomyces* spp. *J Bacteriol* 199:e00465-16. <https://doi.org/10.1128/JB.00465-16>.

Editor Piet A. J. de Boer, Case Western Reserve University School of Medicine

Copyright © 2016 American Society for Microbiology. All Rights Reserved.

Address correspondence to Katsuya Fuchino, katsuya.fuchino@biol.lu.se.

† Deceased.

and bursting of the cell (2). With hyperosmotic stress, the direct accumulation of solutes can prevent the outflux of water, loss of turgor pressure, and dehydration of the cytoplasm (3, 4). Typically, the immediate response involves the influx of K^+ ions, which later are replaced by compatible organic solutes, like proline or glycine betaine (1, 3). On a longer time scale of several minutes to hours, the adaptation to osmotic stress needs transcription/translation and the production of new proteins (1). Important regulatory pathways involved in the reprogramming of the physiology of the cell have been elucidated in *Escherichia coli* and other model bacteria (5–7). Studies of the regulation of bacterial stress responses are now increasingly being complemented by imaging approaches that enable studies of single cells *in situ* under osmotic stress. Such investigations have resulted in new insights into turgor pressure, cell growth, cell wall synthesis machineries, cytoskeleton, chromosome topology, and physical properties of the cytoplasm (8–11).

An important factor that is likely to affect the cell's physiology during hyperosmotic stress is the hydration status of the cytoplasm. A single-cell study proposed that excessive dehydration of the cytoplasm might be the reason why a severe osmotic upshift causes *Escherichia coli* cells to spend a long time in a lag period of complete growth arrest, being apparently unable to initiate the adaptation program, which would otherwise start in minutes following a more gradual or milder osmotic upshift (12). They showed that loss of water in such cells caused the transition of the cytoplasm into a gel-like state, rendering the larger molecules of the cell, such as proteins and DNA, virtually immobile, and inhibiting most cellular processes (12). A glass-like state of the cytoplasm of cells in the imbalanced state directly after a sudden osmotic upshift was also suggested by Parry et al. (13).

Dehydration of the cytoplasm after hyperosmotic shock results in a decrease in turgor. Previous measurements in batch cultures indicated that turgor pressure decreased with increasing medium osmolality in *E. coli*, thus implicating decreased turgor as a possible reason for slower growth at higher osmolality (3, 14, 15). However, a decrease in turgor pressure in *E. coli* cells did not immediately prevent the incorporation of new peptidoglycan (8). Pilizota and Shaevitz also showed that turgor pressure is not responsible for the slow growth of *E. coli* on high-osmolality media (16). However, in the Gram-positive bacterium *Bacillus subtilis*, turgor pressure was suggested to be essential for cell growth (10). To understand the fundamental relationships between osmotic stress, growth, and turgor pressure in bacteria, more research is needed on bacteria with contrasting cell wall structures and growth strategies.

In this study, we have asked how hyperosmotic shock perturbs the growth machinery in *Streptomyces coelicolor*, a Gram-positive bacterium that grows by building its cell wall in restricted zones at the cell poles. The majority of other rod-shaped bacteria, including *E. coli* and *B. subtilis*, employ the actin-like MreB cytoskeleton to direct the incorporation of new peptidoglycan along the lateral wall of the cell (17). In contrast, many members of the *Actinobacteria* exhibit a mode of polar growth that is independent of MreB and instead requires the coiled-coil protein DivIVA, which forms multi-protein complexes at growing cell poles termed polarisomes (18). Corynebacteria and mycobacteria are rod-shaped actinobacteria and grow at cell poles that are generated by cell division. On the other hand, streptomycetes generate the growing cell poles (or hyphal tips) *de novo*, independently of cell division, leading to their characteristic growth as filamentous and branching hyphal cells (19). Assembly of polarisomes is critical for the initiation of polar growth and formation of new hyphal branches in *Streptomyces*, and it is mainly determined by a polarisome-splitting mechanism. Small foci of DivIVA are budded off from established polarisomes at hyphal tips, deposited along the lateral wall, and used as seeds for the development of new growth zones (20, 21). The mechanisms that regulate the hyphal growth machinery in *Streptomyces* are poorly understood, but it has been shown that phosphorylation of DivIVA by the eukaryotic-like serine/threonine kinase AfsK is an important factor to modulate the polar growth and branching, particularly in response to inhibitors of peptidoglycan synthesis (22). The essential DivIVA recruits also two other coiled-coil proteins that are

involved in polar growth of *Streptomyces* hyphae. Scy colocalizes with DivIVA and has been suggested to have scaffolding role in the polarisome; the protein FilP can form intermediate filament-like filaments *in vitro* and has been proposed to form a stress-bearing network to provide mechanical support to the cell wall immediately behind the hyphal tip (22–27).

Several studies have previously shown that sigma factor σ^B is an important master regulator for coping with osmotic stress in *S. coelicolor* (7, 28, 29). However, it is yet poorly understood how sudden osmotic shock influences polar growth of *Streptomyces* spp. or other actinobacteria. It has been suggested that mechanical expansion by turgor is a critical driving force in apically growing cells, eukaryotic as well as prokaryotic (30, 31). Further, polar growth of *Streptomyces* hyphae is fundamentally different from the growth modes of conventional model bacteria and is directed by self-assembling coiled-coil proteins rather than the actin-like MreB and tubulin-like FtsZ cytoskeletons. Here, we show that sudden hyperosmotic stress causes dynamic changes in cell growth, the subcellular distribution of coiled-coil cytoskeletal proteins, and their relationships to cell wall assembly, nucleoid condensation, and turgor pressure.

RESULTS

Hyperosmotic stress triggers reprogramming of cell polarity and redistribution of polar growth sites in *Streptomyces*. In order to observe morphological responses of *Streptomyces* hyphae to hyperosmotic stress, we performed time-lapse imaging of *S. coelicolor* hyphae that were first grown on cellophane discs on a yeast extract-malt extract (YEME) medium without sucrose and then transferred onto a YEME medium with sucrose in a microscope growth chamber (leading to a measured increase in osmolality of 1.33 osmol/kg). It is to be noted that *S. coelicolor* does not catabolize sucrose, and any contaminating monosaccharides in the sucrose preparation would be insignificant in relation to the glucose (10 g/liter) that is already present in the YEME medium (32). Control experiments showed that transfer onto an identical medium without sucrose did not cause any disturbance in the growth or morphology of the hyphae (see Fig. S1 in the supplemental material). Further, after adaptation, *S. coelicolor* grew well in the sucrose-containing YEME medium, which had a total osmolality of 1.44 osmol/kg.

After the osmotic upshift, growth of the *S. coelicolor* hyphae ceased completely for 2 to 3 h (Fig. 1A). After this lag period, growth was resumed but displayed an unexpected pattern. Multiple new branches emerged from the lateral hyphal wall almost simultaneously, while no regrowth occurred at the majority of the existing tips (77% of 322 hyphae exhibited regrowth exclusively at lateral sites, 12% resumed growth at existing tips, and 11% did not regrow). The regrowth from multiple lateral sites on hyphae occurred nearly synchronously throughout the sample (Fig. 1A). These experiments revealed that adaptation to high osmolality involves reprogramming of cell polarity and a pronounced change in the growth pattern of the mycelium. Although the majority of the hyphae managed to adapt to hyperosmotic stress and reinstate growth, 11% of the hyphae did not regrow. Most of these nongrowing hyphae stayed intact during the observation, but in some cases, we observed swelling and bursting of the tips shortly before or after the initiation of regrowth of other hyphae. When treated with a lower osmotic upshift (to a lower sucrose concentration, leading to a difference in osmolality of 0.73 osmol/kg), 59% of 141 hyphae still exhibited reprogramming of cell polarity, and the higher percentage of hyphae (28% of 141 hyphae) regrew at existing tips, while 13% of the hyphae did not regrow during the observation.

Sucrose is a nonionic osmolyte, and we wondered whether NaCl could trigger a similar response. An osmotic upshift by 0.97 osmol/kg into an NaCl-containing medium caused the cessation of hyphal growth for about 2 to 3 h, followed by reprogramming of cell polarity (Fig. 1B), similarly to the case with the sucrose-mediated upshift of 1.33

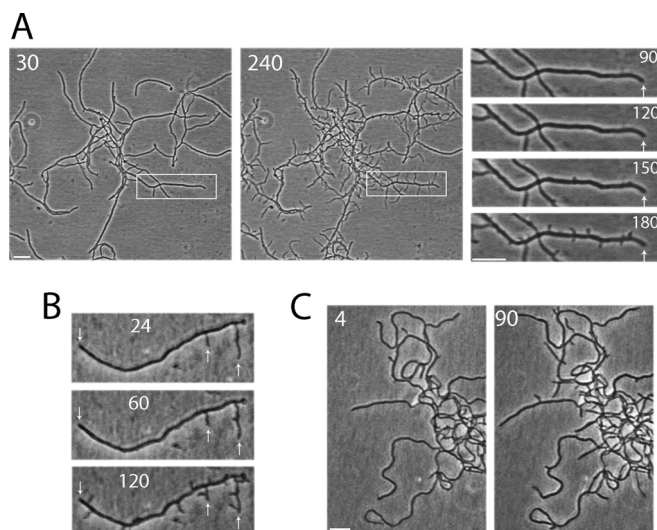


FIG 1 Osmotic upshift causes a long period of growth arrest and subsequent reprogramming of cell polarity in *S. coelicolor*. (A) Strain M145 was grown on the surface of a cellophane membrane positioned on YEME medium without sucrose for 8 h, transferred to YEME with sucrose, resulting in an osmotic upshift of 1.33 osmol/kg, and monitored by phase-contrast microscopy and time-lapse imaging. Osmotic upshift caused a growth arrest for approximately 3 h, after which hyphae regrew by synchronized formation of multiple branches. No regrowth occurred at the existing tips, indicated by arrowheads, indicating reprogramming of cell polarity. (B) Osmotic upshift of 0.97 osmol/kg by ionic osmolyte NaCl caused a similar response as in panel A. (C) Osmotic downshift of 1.33 osmol/kg by sucrose caused a growth arrest but not reprogramming of polarity. Numbers in the panels A to C designate minutes after an osmotic shock. Scale bars correspond to 8 μm .

osmol/kg. These results indicate that the increase in growth medium osmolality rather than a specific solute property triggers the change in growth pattern.

To further examine if regrowth by reprogramming of cell polarity is specific to hyperosmotic stress, we subjected the hyphae to hypo-osmotic (downshift of 1.33 osmol/kg from medium with to medium without sucrose) and acid stress (from pH 6.7 to 4.3) using procedures similar to those described above. Upon an osmotic downshift, hyphal growth stopped for about 30 min and then resumed at the existing tips, showing a clear contrast to the hyperosmotic stress response (Fig. 1C). Acid stress also caused the cessation of growth and a lag period of up to 4 h. However, despite a long lag, regrowth occurred at existing tips (see Fig. S2 in the supplemental material). This shows that reprogramming of cell polarity is not caused by a long growth arrest but is a specific response elicited by high medium osmolality.

To test if the response is conserved in different *Streptomyces* species, we performed osmotic upshift experiments with *Streptomyces venezuelae*, a phylogenetically distant species from *S. coelicolor*. Upon a sucrose-mediated upshift of 1.14 osmol/kg, *S. venezuelae* responded similarly to *S. coelicolor* (see Fig. S3 in the supplemental material), indicating that rearrangement of the polar growth pattern upon hyperosmotic stress is not specific to *S. coelicolor* only.

To summarize, osmotic upshift in the growth medium caused a prolonged lag period and a dramatic change in the polar growth pattern of *Streptomyces* hyphae. Most prestress tips became permanently arrested, and regrowth occurred via simultaneous formation of multiple new lateral branches. Hypo-osmotic and acid stresses also caused a growth arrest but no redistribution of polar growth sites. Thus, it appears that hyperosmotic stress exerts a specific effect on the cell wall growth patterns in *Streptomyces*.

DivIVA and FilP maintain their localizations throughout the lag period and delocalize from the arrested tips before regrowth. Since an osmotic upshift triggered a reprogramming of cell polarity, the localization of DivIVA-containing polarisomes was investigated using a merodiploid *S. coelicolor* strain carrying *divIVA* and

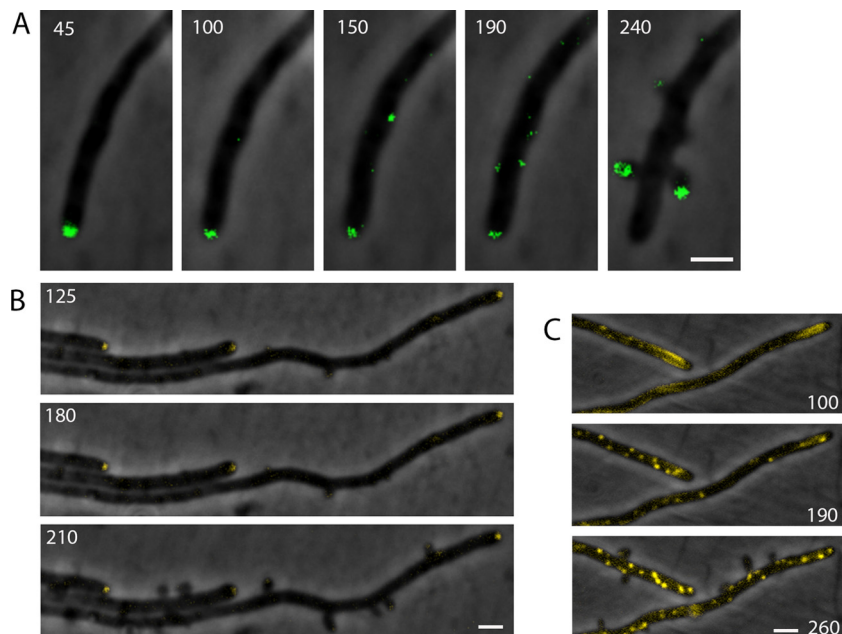


FIG 2 DivIVA and FilP, but not Scy, relocalize before growth resumes after an osmotic upshift. (A) DivIVA-EGFP localization in strain K112 at indicated times during hyperosmotic stress. Significant amounts of DivIVA-EGFP were retained in polar clusters during the first 100 min of the lag period. Most polar foci had disappeared by the time growth resumed. Shown is an overlay of DivIVA-EGFP fluorescence (green) and phase-contrast images. (B) Scy-YPet localization in strain NA1157 during hyperosmotic stress response. Scy-YPet remained at the hyphal tips during the lag phase and even after growth resumed. Shown is an overlay of Scy-YPet fluorescence (yellow) and phase-contrast images. (C) FilP-YPet localization in the strain NA1079 during hyperosmotic stress response. FilP-YPet remained in the apical gradients during the lag phase, which collapsed into foci just before growth resumed. Shown is an overlay of FilP-YPet fluorescence (yellow) and phase-contrast images. Numbers in the figures designate minutes after an osmotic upshift of 1.33 osmol/kg. Scale bars correspond to 2 μ m.

divIVA-egfp at the chromosomal *divIVA* locus (K112). DivIVA is an essential determinant of polar growth and recruits cell wall synthesis machinery into polar complexes called polarisomes (21, 23). Similarly to the wild-type strain, transfer of K112 onto a high-osmolality medium containing sucrose caused cessation of growth for 2.5 to 3 h. However, only 40% of the K112 hyphae ($n = 324$) regrew exclusively at lateral sites (corresponding value for M145 was 77%), and 59% continued to grow at the existing tips (corresponding figure for M145 was 12%). One percent of the K112 hyphae did not regrow. Excessive amounts of the DivIVA/DivIVA-enhanced green fluorescent protein (EGFP) complex or the molecular nature of DivIVA-EGFP in K112 might have caused its deviating behavior upon hyperosmotic shift. However, since 40% of the K112 hyphae still exhibited complete reprogramming of cell polarity, we investigated the localization of DivIVA-EGFP in these hyphae. Surprisingly, 99% of such hyphae retained a significant amount of their apical DivIVA-EGFP for at least 100 min after upshift (Fig. 2A). DivIVA-EGFP foci gradually decreased in intensity and disappeared before lateral regrowth became visible in 78% of the hyphae (Fig. 2A), but 22% retained their apical DivIVA-EGFP foci throughout the observation period, despite their inability to grow from this cell pole (percentages refer to all hyphae that exhibited reprogramming of cell polarity). Since the EGFP tag appeared to affect normal DivIVA function, as was also indicated in the original publication (23), we aimed to confirm our results for the wild-type strain using immunofluorescence microscopy (IFM) with anti-DivIVA antibodies. The IFM images of M145 hyphae treated with same osmotic upshift showed that DivIVA persisted at the prestress tips in the lag phase, after the arrest of tip extension (see Fig. S4 in the supplemental material). However, due to difficulties in obtaining appropriately permeabilized cells, we did not obtain immunostaining data on DivIVA subcellular localizations 30 to 60 min before the regrowth.

DivIVA tip localization in the stressed hyphae was a surprising finding, because the presence of apical DivIVA foci is related to active growth (21). Perhaps a loss of another polarisome component rendered the tips inactive, despite the presence of DivIVA? With that in mind, we studied how osmotic upshift affects the localization of Scy and FilP, two coiled-coil proteins that interact with DivIVA and have a role in polar growth (25, 26, 33). Functional Scy-YPet (a C-terminal fusion of Scy to a yellow fluorescent protein) stayed at the arrested tips throughout the lag period and persisted there even after lateral regrowth had started in strain NA1157 (Fig. 2B). Scy is a large coiled-coil protein, an important component of the polarisomes, and is suggested to form a polar scaffold which might stabilize the DivIVA structures (26). Although it cannot formally be excluded that tagging of Scy with YPet may have influenced the stability of Scy foci, our data indicate that the growth arrest of the main hyphal tips and the apparent inactivity of their polarisomes are not caused by an absence of Scy.

FilP is an intermediate filament-like protein that is recruited by DivIVA to the apical parts of hyphae, where it assembles into cytoskeletal networks that confer mechanical support (25). The localization of the FilP cytoskeleton has been visualized as apical gradients that start just behind the polarisomes (25). The apical gradients of FilP cytoskeleton, which were visualized by FilP-YPet in a merodiploid *Streptomyces* strain NA1079 (*filP* and *filP-YPet*), persisted during the lag period but collapsed into foci in all observed hyphae just before lateral regrowth started (Fig. 2C). Since FilP-YPet is not functional on its own, we aimed to verify FilP localization during the stress by IFM on the wild-type strain. The IFM images showed that FilP remained as apical gradients for at least 10 min after an osmotic upshift (see Fig. S4B in the supplemental material), after which we were unable to obtain appropriately permeabilized hyphae for IFM analysis.

To further test the roles of FilP and Scy in the reprogramming of polar growth after hyperosmotic shock, we investigated the response of mutants lacking these proteins. Strains lacking *scy* (NA336) or *filP* (NA883) exhibited responses to osmotic upshift similar to those of the wild type, in the sense that regrowth occurred as multiple lateral branches (see Fig. S5 and S6 in the supplemental material), showing that neither of these two coiled-coil proteins are required for complete reprogramming of cell polarity.

Phosphorylation of DivIVA by AfsK is not involved in reprogramming of cell polarity during hyperosmotic stress. The serine/threonine protein kinase AfsK has been shown to phosphorylate DivIVA and modulate the polar growth and branching pattern of *Streptomyces* vegetative mycelium, including the stimulation of hyperbranching by a constitutively active form of the kinase (22). Thus, *afsK* was an obvious candidate to investigate for a role in reprogramming of cell polarity in hyperosmotic response. However, an *afsK* mutant strain (M1101) responded in an identical manner to osmotic upshift as strain M145: a growth-arrest period of 2.5 to 3 h was followed by extensive and simultaneous regrowth at lateral sites, whereas no growth occurred at prestress tips of the majority of hyphae. Interestingly, *de novo* branch formation occurred also at high frequency in the normally long branchless apical regions of the *afsK* mutant strain (Fig. 3B). These results show that AfsK is not required for the reprogramming of cell polarity during the hyperosmotic stress response. Western blot analysis of samples taken during an osmotic upshift in liquid cultures of *afsK* mutant M1101 showed no significant phosphorylation of DivIVA during the stress response (Fig. 3A). Phosphorylation of DivIVA is manifested as the appearance of more slowly migrating additional bands in SDS-PAGE (22), shown in the positive control (Fig. 3A, lane 2, Bm145). This result indicates that DivIVA is not significantly phosphorylated by any other kinase under these conditions. The data also show that the amount of DivIVA increases by about 60% in the later stages of the osmotic adaptation period, just before regrowth becomes visible in the microscope, indicating that *de novo* synthesis of DivIVA is involved in the formation of new polarity centers after an osmotic upshift (Fig. 3A).

We also tested a panel of mutants known to be affected in the adaptation to osmotic stress and found that all mutants behaved similarly to the wild type regarding polar reprogramming and the timing and pattern of lateral regrowth. Mutations

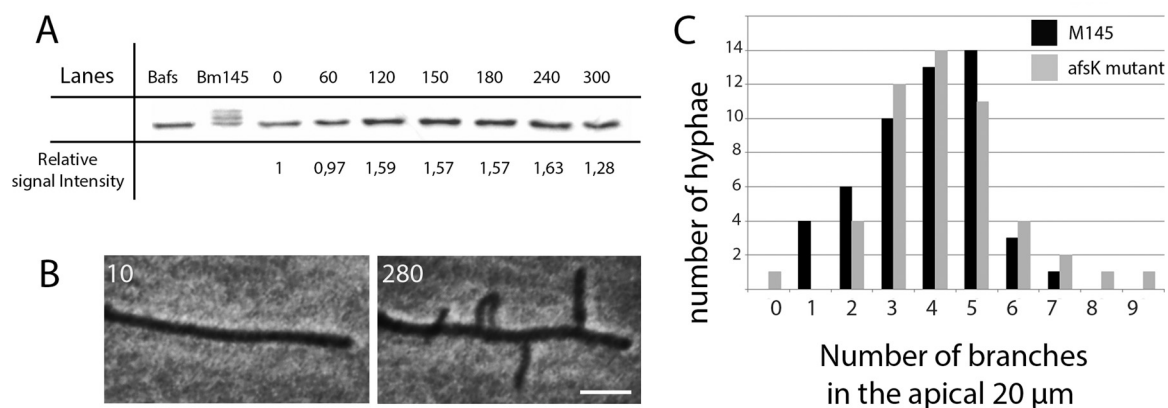


FIG 3 AfsK is not involved in reprogramming of cell polarity. (A) Western blot of cell lysates of the *afsK* mutant (strain M1101) hyphae collected throughout an osmotic upshift experiment, showing the amount and phosphorylation of DivIVA (manifested as additional bands, seen in lane Bm145). Numbers in lanes designate minutes after an upshift. Bacitracin treatment causes phosphorylation of DivIVA in *S. coelicolor afsK*⁺ strain M145 and was used as a positive control (lane Bm145) to show the mobility-shifted bands of phosphorylated DivIVA (22). The *afsK* mutant M1101 does not phosphorylate DivIVA in response to bacitracin and is used here (lane Bafs) to show the mobility of unphosphorylated DivIVA (22). (B) Phase-contrast images of the *afsK* mutant strain M1101 before and after regrowth following an osmotic upshift. Numbers in the figure designate minutes after the osmotic upshift. Scale bar corresponds to 5 μm. (C) Diagram showing the frequency of new branches per 20 μm in the apical region of hyphae in M145 and M1101, measured 30 min after regrowth in hyphae that had first been subjected to an osmotic upshift and then spent about 2.5 h in the adaptation phase before they started growth again.

concerned the following genes: *osaB* and *osaC*, encoding known osmotic stress regulators (28, 34); *sigB* and *sigH*, encoding sigma factors (35, 36); and *glxA*, encoding a galactose oxidase-like protein required for osmotic adaptation (37). Since we also observed chromosome hypercondensation after osmotic upshift (see below), mutants of *ddbA*, encoding a histone-like protein upregulated in osmotic stress, (38) and *hupS*, encoding a histone-like protein needed for chromosome compaction during sporulation (39), were also tested and found to behave similarly to the wild type (data not shown).

Chromosomes hypercondense in response to osmotic upshift. Our results revealed that there is a long lag period before growth resumes after the osmotic upshift. Transient hypercondensation of chromosomes has recently been demonstrated to occur during the lag period caused by osmotic upshift in *E. coli* (9), but in *Streptomyces* spp., this phenomenon was not observed in cells already adapted to growth on high-osmolality medium (40). In order to visualize nucleoid structure in live cells throughout the osmotic adaptation, we used a strain in which the nucleoid-associated protein HupA was fused to EGFP (K306). We observed that chromosomes were severely condensed in cells subjected to osmotic upshift (Fig. 4). We then attempted to perform time-lapse imaging to visualize the dynamics of nucleoid condensation during the entire upshift experiment but found that the strains carrying nucleoid-associated protein tagged with EGFP were subjected to significant phototoxicity, manifested in

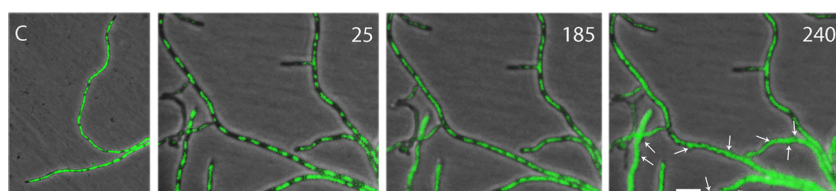


FIG 4 Chromosomes hypercondense after transfer to high-osmolality medium and decondense shortly before initiation of regrowth. Nucleoid localization during hyperosmotic stress response. Images are overlays of HupA-EGFP fluorescence (green) and phase-contrast images at indicated times during the adaptation following hyperosmotic shift of the *S. coelicolor* strain K306 (labeled as 25, 185, or 240). The panel labeled “C” shows hyphae growing on cellophane on YEME medium without sucrose, before exposed to osmotic stress. Other panels are labeled with time in minutes after the osmotic upshift. Arrowheads indicate sites of regrowth that occurred just after 240 min. Scale bar corresponds to 4.4 μm.

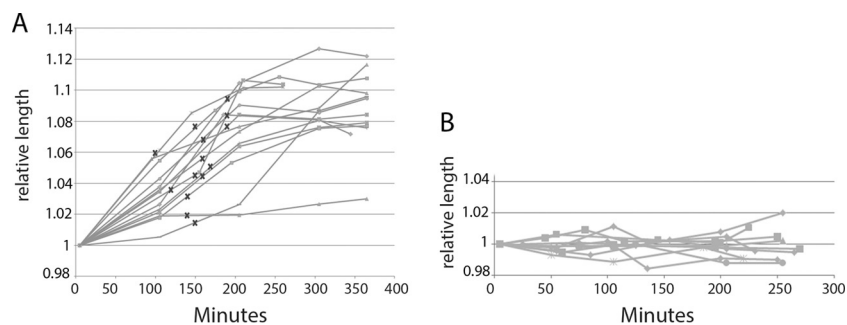


FIG 5 Stretching of hyphae during the lag phase indicates that recovery of turgor pressure. (A) Relative lengths of defined segments (between branches) in 14 *S. venezuelae* hyphae at indicated times after an osmotic upshift of 1.14 osmol/kg in sucrose-containing YEME medium (time zero). The first measurement was possible at 5 min after the upshift, required for transfer of the hyphae to the growth chamber and setting up the time-lapse microscopy. The initiation of regrowth for each hypha is indicated by "X." (B) Control experiments for panel A showing relative lengths of defined segments (between branches) in 10 *S. venezuelae* hyphae transferred from low-osmolality YEME medium to the same medium in the microscope growth chamber without any osmotic upshift or growth arrest, showing that the lengths of internal segments do not change during growth.

these experiments as an inability of exposed hyphae to regrow, while nonexposed cells in the same sample regrew normally. Nevertheless, an analysis of data from several individual time-lapse experiments with infrequent exposures revealed that the chromosomes condense soon after the osmotic upshift and decondense just before regrowth occurs (Fig. 4). These data, in combination with results shown above, suggest that during adaptation to high osmolality the cells first enter a state with no growth, tightly condensed chromosomes, and static nonoperational polarisomes, followed by a dynamic period before regrowth occurs, during which the chromosomes decondense, new polarisome components are synthesized (shown for DivIVA, Fig. 2), and the old polarisomes are disassembled and redistributed to new polarity centers.

Turgor pressure is restored in a slow and gradual fashion during the lag period, and no growth occurs before substantial recovery of turgor. Hyperosmotic stress is likely to cause outflow of water from the cells, resulting in a loss of turgor pressure. However, it is not known whether this is the case also in *Streptomyces* species. It was not feasible for us to directly measure the cellular turgor of *Streptomyces* hyphae by the methods available for measuring turgor of filamentous fungi (41), but we noticed that hyphae expand during the adaptation. Because the hyphae had firmly adhered to the cellophane, expansion often caused detachment and a sudden whip-like straightening motion of apical regions, or curving of some internal regions of hyphae. We reasoned that since *Streptomyces* vegetative hyphae grow strictly via tip extension, elongation of nonapical mycelial segments can only occur due to mechanical stretching by a change in their turgor. Thus, measuring the lengths of nonapical hyphal segments following an osmotic upshift will give an indication of changes in turgor. To avoid firm attachment of cells to the substrate, hyphae were grown in liquid low-osmolality medium and transferred to solid high-osmolality medium for microscopy. Also, since *S. coelicolor* forms tight mycelial pellets in YEME without sucrose that are not amenable to microscopy, we used *S. venezuelae*, which exhibits dispersed growth and responds similarly to *S. coelicolor* to osmotic upshift (see Fig. S3 in the supplemental material). Internal hyphal segments between two branches, serving as landmarks, were manually measured from time-lapse images collected during osmotic upshift. The immediate response to the osmotic shock could not be monitored, since measurements could not start until a few minutes after hyphae had been exposed to the high-osmolality medium. However, during the adaptation period, the length of the measured segments indeed increased in a linear fashion by 8.8% on average (standard deviation, 2.1%) (Fig. 5A). No increase in hyphal length was observed when the cells were transferred to low-osmolality agar without interruption of growth (Fig. 5B), confirming that the observed change in hyphal length after osmotic upshift reflects a

slow and gradual stretching of hyphae due to increased turgor pressure, following an immediate loss of turgor upon exposure to the stress. Interestingly, no growth occurred before turgor pressure had recovered significantly, although full stretching of the hyphae was reached, and then maintained, sometime after growth had resumed. Our data show that there is loss of turgor after osmotic upshift, hyphae experience significant dehydration of the cytoplasm, and rehydration and recovery of turgor occur slowly.

Rapid inactivation of hyphal tips upon hyperosmotic stress. In order to better understand why cells needed the extended lag period to adjust their physiology to the higher osmolality, we performed osmotic reversal experiments: hyphae were transferred to the high-osmolality medium (1.33-osmol/kg upshift), incubated for different time intervals (ranging from 1 to 65 min), transferred back to low-osmolality (no-sucrose) medium in the growth chamber, and monitored by time-lapse microscopy. Exposure for 1 min to high-osmolality medium resulted in a mixed pattern of regrowth (see Fig. S7 in the supplemental material). Hyphae that had spent 10 min or more on the high-osmolality medium resumed growth approximately 30 to 50 min after transfer to low-osmolality medium and exhibited complete reprogramming of cell polarity, i.e., most of the hyphae resumed growth by establishment of new branch sites (see Fig. S7). The timing of regrowth did not depend on the time spent on high-osmolality medium. Thus, irreversible inactivation of the cell wall growth zones at existing hyphal tips occurs during the first 10 min after exposure to hyperosmotic shock and is not a consequence of a prolonged growth arrest.

DISCUSSION

An unexpected finding in our study was that external osmotic upshift triggers a dramatic rearrangement and relocalization of cell wall biosynthetic machineries in *Streptomyces*, a phenomenon that, to our knowledge, has not previously been reported. What could be the underlying mechanism for the reprogramming of cell polarity? Growth polarity in *Streptomyces* is determined by DivIVA, which forms large cytoskeleton-like assemblies called polarisomes at the tips of the hyphae and recruits, directly or indirectly, cell wall synthesis machinery and other proteins needed for growth (21, 23, 24). Consistently, the initiation of lateral branches that occurred during recovery from osmotic shock was preceded by the appearance of new polarisomes at the lateral branch points and a gradual decrease in intensity of the original apical DivIVA focus (Fig. 2A). This redistribution of polarisomes was not mediated by any of the tested genes that are known to be involved in regulating cell polarity or the response to osmotic shock in *S. coelicolor* (*scy*, *filP*, *afsK*, *osaA*, *osaB*, *sigB*, and *sigH*). Thus, the underlying mechanism that causes the inactivation, gradual dismantling, and redistribution of polarisomes in response to osmotic shock is not known. Interestingly, the presence of DivIVA-EGFP in addition to DivIVA in strain K112 caused a clear difference in the response to osmotic stress compared to the strain with only wild-type DivIVA, and it enabled regrowth of more than half of the prestress tips. In fact, K112 was the only strain in a panel of tested mutants (Table 1) that showed a different behavior from the wild type in polar reprogramming, indicating that DivIVA is involved in the mechanism. It is tempting to speculate that the GFP tag stabilized the DivIVA foci, making them less susceptible to osmotic shock-induced disassembly, thus partially preventing inactivation of the existing polarisomes and reprogramming of cell polarity.

The inactivation of growth zones at existing hyphal tips is likely related to the loss of turgor upon the osmotic shock. Our osmotic reversal experiments showed that the loss of turgor *per se*, which should take place in seconds after the shock, was insufficient to cause irreversible inactivation of the tips (but note that we could not monitor whether the hyphae stopped extension immediately or with some delay). However, less than 10 min of osmotically induced growth arrest caused most existing tips to lose their growth competency and be abandoned, leading instead to the formation of new branches where regrowth occurred. The regrowth did not occur until a turgor was partially restored. These findings would be consistent with a critical role of turgor

TABLE 1 Strains and plasmids used in this study

Strain/plasmid	Genotype/description ^a	Source or reference
Strains		
<i>S. coelicolor</i>		
DSCO2837 Δ glxA	M145 glxA::Tn5062	37
DSCO5749	M145 osaB::Tn5062	28
DSCO5747-1	M145 osaC::Tn5062	28
K112	M145 divIVA ⁺ ::pKF59[Φ (divIVA-egfp)]	23
K306	M145 hupA::pKF290[hupA-egfp]	39
M1101	M600 Δ afsK::[aac-(3)-IV oriT]	22
M145	Prototrophic, SCP1 ⁻ SCP2 ⁻	32
M145 Δ sigB	M145 Δ sigB::[aac-(3)-IV oriT]	28
M145 Δ sigH	M145 Δ sigH::thio	51
M145 ddbA	M145 ddbA::Tn5062	38
M600	Prototrophic, SCP1 ⁻ SCP2 ⁻	32
NA336	M145 scy::[aac-(3)-IV oriT]	33
NA883	M145 filP::[FRT]	25
NA1079	M145 attP _{ϕC31} ::pNA1054([filP-yPet])	This study
NA1157	M145 scy::scy-yPet	This study
K304	M145 hupS::hyg	39
<i>S. venezuelae</i>		
ATCC 10712	Wild type	Lab stock
<i>E. coli</i>		
DH5 α	Cloning strain	Lab stock
DY380	DH10B λ cl857 Δ (cro-bio) < > tet	52
ET12567/pUZ8002	dam-13::Tn9 dcm-6 hsdM, carries RK2 derivative with defective oriT for plasmid mobilization	32
Plasmids		
pNA1054	pSET152 containing filP-yPet	This study
pSET152	Mobilizable vector that integrates at ϕ C31 attB site in <i>S. coelicolor</i> , Apra ^r	53

^aApra^r, ●●●.

pressure in hyphal growth of *Streptomyces*, similar to several eukaryotic tip-growing organisms that are known to require turgor to drive tip extension (41, 42). However, we cannot exclude that possibility that other aspects of osmotic stress, for example, dehydration of the cytoplasm, cause the growth arrest, and that cell wall synthesis could continue for some time even in the absence of turgor. That would be reminiscent of the situation in the Gram-negative bacterium *E. coli*, where two recent reports show that turgor is not required for cell wall expansion following osmotic shock (8, 16).

New branches are initiated by the establishment of new zones for peptidoglycan synthesis at assemblies of DivIVA at the lateral hyphal wall (21). Based on time-lapse imaging and mathematical modeling, it was recently found that new branch sites are established by a polarisome-splitting mechanism in *S. coelicolor* (20). Small fragments of the DivIVA polarisomes at growing hyphal tips are broken off and deposited on the lateral wall. The model suggests that these daughter polarisomes grow by attracting diffusible DivIVA subunits until a critical size is achieved, at which a new branch can be initiated. The majority of branching events during normal growth occur from such split polarisomes rather than by nucleation of new DivIVA foci from soluble subunits (20). Thus, the lateral branches that emerge during regrowth after osmotic upshift may also emanate from daughter polarisomes that have been deposited along the lateral wall already during growth before exposure to the stress. However, the number of lateral branches formed during the regrowth period is higher than what is seen under prestress conditions (see Fig. 1A). There are three possibilities for how these additional branches arise. First, it is possible that more daughter polarisomes are actually deposited than are normally used for branching under normal growth conditions. Some of the small polarisomes that break off from the main tip and are left on the lateral wall

may under normal conditions disintegrate or fail to recruit sufficient DivIVA molecules to initiate a branch. When the main tip is arrested upon osmotic shock, the released DivIVA from arrested tips may allow a larger number of daughter polarisomes to grow in size and start new branches. Second, the released DivIVA from arrested tips may also, in combination with newly synthesized molecules, lead to a sufficiently high cytoplasmic concentration of DivIVA to promote *de novo* nucleation of new polarisomes. Finally, a third possibility would be that larger complexes of DivIVA may dissociate from the arrested hyphal tips and then reattach to the membrane elsewhere in the cell. It is currently not possible to judge to what extent these different mechanisms contribute to the increased number of lateral branches that are seen during regrowth from osmotic shock.

The adaptation period before regrowth occurred was long and lasted 2 to 3 h after the hyperosmotic shock. The reason is likely because loss of cellular water would not only reduce the turgor pressure but also cause a profound change in the cytoplasmic environment. It is known that *E. coli* cells enter a prolonged lag period after a severe osmotic upshift, and the growth arrest period can last for hours or even indefinitely (12, 15). It has been proposed that the time until recovery of growth is determined by the recovery of the ability of the proteins to diffuse in the cytoplasm (12). Indeed, the diffusion constants of GFP in individual cells suffering an osmotic upshift have been shown to decrease by more than an order of magnitude, both in Gram-negative *E. coli* and Gram-positive *Lactococcus lactis* (12, 43, 44). Konopka et al. found that in severely plasmolyzed *E. coli* cells, diffusion of GFP was unexpectedly slow and could not be explained by molecular crowding only (12). Interestingly, it has been shown more recently that the bacterial cytoplasm displays properties that are characteristic of glass-forming liquids and can shift between liquid-like and glass-like states (13). These findings offer a possible explanation to why the hyphae entered a long cell-biologically static state without any growth. Several of our observations are consistent with the idea that an osmotic upshift caused drastically limited diffusion and cessation of normal physiological processes. For example, osmotic reversal experiments indicated that most of the growing hyphal tips were inactivated during the first 10 min on high-osmolality medium, but both the DivIVA-EGFP foci and the FilP cytoskeletal structures appeared to be immobile for the first 100 min after osmotic upshift and disappeared during the dynamic adaptation period before regrowth. Mika et al. have shown that a 15% reduction in cell volume in *L. lactis* upon osmotic upshift was accompanied by a drop of the diffusion coefficient by almost two orders of magnitude (43). It might be challenging for the cell without fluidization of the cytoplasm to recover from the static state.

To our knowledge, only a few studies have addressed dynamic changes in the bacterial nucleoid structure during exposure to osmotic change. Cagliero and Jin showed in single-cell investigations that approximately 10 min after osmotic upshift, the nucleoids of *E. coli* became hypercondensed, and most of the RNA polymerase molecules dissociated from the nucleoid (9). We have shown here that chromosomes of *Streptomyces* spp. also hypercondensed within the first 20 min after exposure to high osmolality, stayed in the condensed state throughout the lag period, and decondensed shortly before growth resumed (Fig. 4). Osmotic upshift has also been shown to cause chromosome condensation in various types of eukaryotic cells (45, 46). Recently, Irianto et al. showed that in human chondrocytes, hyperosmotic conditions induced rapid and reversible chromatin condensation, and the authors propose that this process is caused directly by physicochemical factors rather than by the specific action of cytoskeletal elements or other DNA-associated proteins (47). Our demonstration of chromatin hypercondensation as a rapid response to osmotic upshift in an organism evolutionarily distant to *E. coli* and human cells supports the idea that cells have evolved mechanisms to cope with hyperosmotic stress. DNA condensation can lead to differential gene expression by silencing most of the genes and allowing the expression of genes located on the surface of the compacted chromosomes (48).

MATERIALS AND METHODS

Bacterial strains, plasmids, and growth media. The strains and plasmids used in this study are listed in Table 1. The general genetic manipulations and culture conditions for *E. coli* are as described in reference 49. *S. coelicolor* and *S. venezuelae* were grown on solid (with 1.5% agar) or liquid yeast extract-malt extract (YEME) medium (32) with or without sucrose, as specified below. The ingredients for YEME medium were dissolved in 1 liter of water instead of making the final volume up to 1 liter as described in reference 32. The measured osmolality of this YEME medium without sucrose was 0.10 osmol/kg. The osmolality of the sucrose-containing YEME medium used for *S. coelicolor* (to which had been added 340 g sucrose/liter of water) was 1.43 osmol/kg. For *S. venezuelae*, we used a sucrose-containing YEME medium with an osmolality of 1.24 osmol/kg. The osmolality of YEME medium containing 0.5 M NaCl was 1.07 osmol/kg. Osmolalities of the growth media were measured using a freezing-point osmometer (Advanced Instruments).

Construction of strains NA1079 and NA1157. For the construction of NA1079, a DNA region containing *filP*-YPet with a 500-bp upstream sequence was PCR amplified using cosmid 8F4::*filP*-YPet as a template (25) and cloned into the shuttle vector pSET152, creating plasmid pNA1054. This construct was verified by DNA sequencing and transformed into *E. coli* strain ET12567/pUZ8002 for conjugation into the *S. coelicolor* strain M145, where the plasmid integrates into the ϕ C31 attachment site in the chromosome. For construction of *Streptomyces* NA1157, *scy* in cosmid 8F4 was first replaced by *scy*-YPet encoding Scy fused to YPet using λ Red mutagenesis, as previously described for *filP*-YPet (25). 8F4::*scy*-YPet was introduced by protoplast transformation (32) into strain M145. Transformants were selected first for incoming cosmid (kanamycin resistance) and in the next step screened for a loss of kanamycin resistance. The presence of *scy*-YPet only in the native *scy* locus in strain NA1157 was confirmed by diagnostic PCR. NA1157 displayed wild-type hyphal morphology, showing that Scy-YPet is a functional fusion protein.

Osmotic shift experiments. For osmotic upshift experiments, *S. coelicolor* was inoculated on the surface of a cellophane membrane placed on solid YEME medium without sucrose (measured osmolality is 0.10 osmol/kg before addition of agar). After growth for 7 to 10 h, a small square was cut out of the cellophane and carefully transferred onto sucrose-containing solid YEME medium (measured osmolality of 1.43 osmol/kg before addition of agar) in a microscope growth chamber, which was made as described previously (21). The medium in the growth chamber was prepared using agarose. For osmotic downshift experiments, *S. coelicolor* was inoculated on the surface of a cellophane membrane placed on solid YEME medium containing sucrose and transferred to the growth chamber containing solid YEME medium without sucrose (causing a 1.33 osmol/kg downshift). Osmotic reversal experiments were performed by first growing the cells for 7 to 10 h on the surface of a cellophane membrane placed on solid YEME medium without sucrose, transferred onto another plate containing YEME medium with sucrose (causing a 1.33-osmol/kg upshift), and incubated for 1, 10, 30, or 65 min, after which the cellophane was transferred to solid YEME medium without sucrose in the microscope growth chamber. For immunostaining and Western blot experiments, the osmotic shift was performed in liquid culture. *S. coelicolor* strain M145 was grown in liquid YEME medium without sucrose for about 12 h. Grown cultures were centrifuged and resuspended in liquid YEME medium with sucrose and incubated for different time intervals (10, 30, 60, 120, 150, and 180 min) before harvesting samples for Western blot analysis or immunostaining. Cultures for immunostaining were grown in media also containing 0.5% glycine. *S. venezuelae* was grown in liquid YEME medium without sucrose overnight, subcultured into same medium, and grown further for 4 to 5 h. One microliter of exponentially growing culture was mounted onto solid YEME medium with sucrose (causing 1.14-osmol/kg upshift) in a microscope growth chamber.

Microscopy techniques. Hyphae were immunostained as described previously (50). Rabbit anti-FilP antiserum (Innovagen, Sweden) or anti-DivIVA antibodies (23) and secondary goat anti-rabbit antibodies conjugated to Alexa Fluor 568 (Thermo Fisher Scientific) were used to visualize FilP or DivIVA. Immunostained and live cells were observed using a Zeiss Axio Imager.Z1 microscope equipped with a 9100-02 electron-multiplying charge-coupled-device (EMCCD) camera (Hamamatsu Photonics) and Volocity three-dimensional (3D) image analysis software (PerkinElmer). Time-lapse imaging was used for osmotic shift experiments, and images were captured every 2 to 10 min. For fluorescence illumination, X-Cite 120 Illumination (Exfo Photonic Solutions) was used. Images were analyzed and processed with Volocity and Photoshop (Adobe). To monitor the stretching of hyphae by turgor pressure, lengths of hyphal segments between two branch points were measured at several time points using the line function in the Volocity software.

Western blotting. Western blot analysis of DivIVA, including harvest of cells by centrifugation and lysis by bead beating, was carried out as previously described in (22), and the results were imaged by the ChemiDoc MP system (Bio-Rad).

SUPPLEMENTAL MATERIAL

Supplemental material for this article may be found at <https://doi.org/10.1128/JB.00465-16>.

TEXT S1, PDF file, 0.7 MB.

ACKNOWLEDGMENTS

We thank Reinhard Krämer for discussing ideas and Ronald Kröger for assistance with measurement of osmolality.

This work was supported by the Swedish Research Council (grant 621-2209-5475), the Carl Trygger Foundation (grant CTS12:33), and the Crafoord Foundation (grant 20140793).

REFERENCES

- Krämer R. 2010. Bacterial stimulus perception and signal transduction: response to osmotic stress. *Chem Rec* 10:217–229. <https://doi.org/10.1002/tcr.201000005>.
- Booth IR. 2014. Bacterial mechanosensitive channels: progress towards an understanding of their roles in cell physiology. *Curr Opin Microbiol* 18:16–22.
- Wood JM. 2011. Bacterial osmoregulation: a paradigm for the study of cellular homeostasis. *Annu Rev Microbiol* 65:215–238. <https://doi.org/10.1146/annurev-micro-090110-102815>.
- Wood JM. 2015. Bacterial responses to osmotic challenges. *J Gen Physiol* 145:381–388. <https://doi.org/10.1085/jgp.201411296>.
- Altendorf K, Booth IR, Gralla J, Greie J-C, Rosenthal AZ, Wood JM. 2009. Osmotic stress. *EcoSal Plus*. <https://doi.org/10.1128/ecosalplus.5.4.5>.
- Schroeter R, Hoffmann T, Voigt B, Meyer H, Bleisteiner M, Muntel J, Jürgen B, Albrecht D, Becher D, Lalk M, Evers S, Bongaerts J, Maurer KH, Putzer H, Hecker M, Schweder T, Bremer E. 2013. Stress responses of the industrial workhorse *Bacillus licheniformis* to osmotic challenges. *PLoS One* 8:e80956. <https://doi.org/10.1371/journal.pone.0080956>.
- Lee E-J, Karoonuthaisiri N, Kim H-S, Park J-H, Cha C-J, Kao CM, Roe J-H. 2005. A master regulator sigmaB governs osmotic and oxidative response as well as differentiation via a network of sigma factors in *Streptomyces coelicolor*. *Mol Microbiol* 57:1252–1264. <https://doi.org/10.1111/j.1365-2958.2005.04761.x>.
- Rojas E, Theriot JA, Huang KC. 2014. Response of *Escherichia coli* growth rate to osmotic shock. *Proc Natl Acad Sci U S A* 111:7807–7812. <https://doi.org/10.1073/pnas.1402591111>.
- Cagliero C, Jin DJ. 2013. Dissociation and re-association of RNA polymerase with DNA during osmotic stress response in *Escherichia coli*. *Nucleic Acids Res* 41:315–326. <https://doi.org/10.1093/nar/gks988>.
- Misra G, Rojas ER, Gopinathan A, Huang KC. 2013. Mechanical consequences of cell-wall turnover in the elongation of a Gram-positive bacterium. *Biophys J* 104:2342–2352. <https://doi.org/10.1016/j.bpj.2013.04.047>.
- Huang KC. 2015. Applications of imaging for bacterial systems biology. *Curr Opin Microbiol* 27:114–120. <https://doi.org/10.1016/j.mib.2015.08.003>.
- Konopka MC, Sochacki KA, Bratton BP, Shkel IA, Record MT, Weisshaar JC. 2009. Cytoplasmic protein mobility in osmotically stressed *Escherichia coli*. *J Bacteriol* 91:231–237.
- Parry BR, Surovtsev IV, Cabeen MT, O'Hern CS, Dufresne ER, Jacobs-Wagner C. 2014. The bacterial cytoplasm has glass-like properties and is fluidized by metabolic activity. *Cell* 156:183–194. <https://doi.org/10.1016/j.cell.2013.11.028>.
- Cayley DS, Guttman HJ, Record MT, Jr. 2000. Biophysical characterization of changes in amounts and activity of *Escherichia coli* cell and compartment water and turgor pressure in response to osmotic stress. *Biophys J* 78:1748–1764. [https://doi.org/10.1016/S0006-3495\(00\)76726-9](https://doi.org/10.1016/S0006-3495(00)76726-9).
- Wood JM. 1999. Osmosensing by bacteria: signals and membrane-based sensors. *Microbiol Mol Biol. Rev* 63:230–262.
- Pilizota T, Shaevitz JW. 2014. Origins of *Escherichia coli* growth rate and cell shape changes at high external osmolality. *Biophys J* 107:1962–1969. <https://doi.org/10.1016/j.bpj.2014.08.025>.
- Errington J. 2015. Bacterial morphogenesis and the enigmatic MreB helix. *Nat Rev Microbiol* 13:241–248. <https://doi.org/10.1038/nrmicro3398>.
- Cameron TA, Zupan JR, Zambryski PC. 2015. The essential features and modes of bacterial polar growth. *Trends Microbiol* 23:347–353. <https://doi.org/10.1016/j.tim.2015.01.003>.
- Flärdh K. 2010. Cell polarity and the control of apical growth in *Streptomyces*. *Curr Opin Microbiol* 13:758–765. <https://doi.org/10.1016/j.mib.2010.10.002>.
- Richards DM, Hempel AM, Flärdh K, Buttner MJ, Howard M. 2012. Mechanistic basis of branch-site selection in filamentous bacteria. *PLoS Comput Biol* 8:e1002423. <https://doi.org/10.1371/journal.pcbi.1002423>.
- Hempel AM, Wang S, Letek M, Gil JA, Flärdh K. 2008. Assemblies of DivIVA mark sites for hyphal branching and can establish new zones of cell wall growth in *Streptomyces coelicolor*. *J Bacteriol* 190:7579–7583. <https://doi.org/10.1128/JB.00839-08>.
- Hempel AM, Cantlay S, Molle V, Wang S-B, Naldrett MJ, Parker JL, Richards DM, Jung Y-G, Buttner MJ, Flärdh K. 2012. The Ser/Thr protein kinase AfsK regulates polar growth and hyphal branching in the filamentous bacteria *Streptomyces*. *Proc Natl Acad Sci U S A* 109:E2371–E2379. <https://doi.org/10.1073/pnas.1207409109>.
- Flärdh K. 2003. Essential role of DivIVA in polar growth and morphogenesis in *Streptomyces coelicolor* A3(2). *Mol Microbiol* 49:1523–1536. <https://doi.org/10.1046/j.1365-2958.2003.03660.x>.
- Flärdh K. 2003. Growth polarity and cell division in *Streptomyces*. *Curr Opin Microbiol* 6:564–571. <https://doi.org/10.1016/j.mib.2003.10.011>.
- Fuchino K, Bagchi S, Cantlay S, Sandblad L, Wu D, Bergman J, Kamali-Moghaddam M, Flärdh K, Ausmees N. 2013. Dynamic gradients of an intermediate filament-like cytoskeleton are recruited by a polarity landmark during apical growth. *Proc Natl Acad Sci U S A* 110:E1889–E1897. <https://doi.org/10.1073/pnas.1305358110>.
- Holmes NA, Walshaw J, Leggett RM, Thibessard A, Dalton KA, Gillespie MD, Hemmings AM, Gust B, Kelemen GH. 2013. Coiled-coil protein Scy is a key component of a multiprotein assembly controlling polarized growth in *Streptomyces*. *Proc Natl Acad Sci U S A* 110:E397–E406. <https://doi.org/10.1073/pnas.1210657110>.
- Bush MJ, Tschowri N, Schlimpert S, Flärdh K, Buttner MJ. 2015. c-di-GMP signalling and the regulation of developmental transitions in streptomycetes. *Nat Rev Microbiol* 13:749–760. <https://doi.org/10.1038/nrmicro3546>.
- Fernández Martínez L, Bishop A, Parkes L, Del Sol R, Salerno P, Sevcikova B, Mazurakova V, Kormanec J, Dyson P. 2009. Osmoregulation in *Streptomyces coelicolor*: modulation of SigB activity by OsaC. *Mol Microbiol* 71:1250–1262. <https://doi.org/10.1111/j.1365-2958.2009.06599.x>.
- Viollier PH, Kelemen GH, Dale GE, Nguyen KT, Buttner MJ, Thompson CJ. 2003. Specialized osmotic stress response systems involve multiple SigB-like sigma factors in *Streptomyces coelicolor*. *Mol Microbiol* 47:699–714. <https://doi.org/10.1046/j.1365-2958.2003.03302.x>.
- Koch AL. 1994. The problem of hyphal growth in streptomycetes and fungi. *J Theor Biol* 171:137–150. <https://doi.org/10.1006/jtbi.1994.1219>.
- Gray DI, Gooday GW, Prosser JI. 1990. Apical hyphal extension in *Streptomyces coelicolor* A3(2). *J Gen Microbiol* 136:1077–1084. <https://doi.org/10.1099/00221287-136-6-1077>.
- Kieser T, Bibb MJ, Buttner MJ, Chater KF, Hopwood DA. 2000. Practical *Streptomyces* genetics. John Innes Centre, Norwich, United Kingdom.
- Bagchi S, Tomenius H, Belova LM, Ausmees N. 2008. Intermediate filament-like proteins in bacteria and a cytoskeletal function in *Streptomyces*. *Mol Microbiol* 70:1037–1050.
- Bishop A, Fielding S, Dyson P, Herron P. 2004. Systematic insertional mutagenesis of a streptomycete genome: a link between osmoadaptation and antibiotic production. *Genome Res* 14:893–900. <https://doi.org/10.1101/gr.1710304>.
- Cho YH, Lee EJ, Ahn BE, Roe JH. 2001. SigB, an RNA polymerase sigma factor required for osmoprotection and proper differentiation of *Streptomyces coelicolor*. *Mol Microbiol* 42:205–214.
- Kormanec J, Sevciková B, Halgasová N, Knirschová R, Rezuchová B. 2000. Identification and transcriptional characterization of the gene encoding the stress-response sigma factor sigma(H) in *Streptomyces coelicolor* A3(2). *FEMS Microbiol Lett* 189:31–38. <https://doi.org/10.1111/j.1574-6968.2000.tb09202.x>.
- Liman R, Facey PD, van Keulen G, Dyson PJ, Del Sol R. 2013. A laterally acquired galactose oxidase-like gene is required for aerial development during osmotic stress in *Streptomyces coelicolor*. *PLoS One* 8:e54112. <https://doi.org/10.1371/journal.pone.0054112>.
- Aldridge M, Facey P, Francis L, Bayliss S, Del Sol R, Dyson P. 2013. A novel bifunctional histone protein in *Streptomyces*: a candidate for structural coupling between DNA conformation and transcription during development and stress? *Nucleic Acids Res* 41:4813–4824. <https://doi.org/10.1093/nar/gkt180>.
- Salerno P, Larsson J, Bucca G, Laing E, Smith CP, Flärdh K. 2009. One of the

- two genes encoding nucleoid-associated HU proteins in *Streptomyces coelicolor* is developmentally regulated and specifically involved in spore maturation. *J Bacteriol* 191:6489–6500. <https://doi.org/10.1128/JB.00709-09>.
40. Facey PD, Hitchings MD, Saavedra-Garcia P, Fernandez-Martinez L, Dyson PJ, Del Sol R. 2009. *Streptomyces coelicolor* Dps-like proteins: differential dual roles in response to stress during vegetative growth and in nucleoid condensation during reproductive cell division. *Mol Microbiol* 73:1186–1202. <https://doi.org/10.1111/j.1365-2958.2009.06848.x>.
 41. Lew RR. 2011. How does a hypha grow? The biophysics of pressurized growth in fungi. *Nat Rev Microbiol* 9:509–518.
 42. Harold FM. 2002. Force and compliance: rethinking morphogenesis in walled cells. *Fungal Genet Biol* 37:271–282. [https://doi.org/10.1016/S1087-1845\(02\)00528-5](https://doi.org/10.1016/S1087-1845(02)00528-5).
 43. Mika JT, Schavemaker PT, Krasnikov V, Poolman B. 2014. Impact of osmotic stress on protein diffusion in *Lactococcus lactis*. *Mol Microbiol* 94:857–870. <https://doi.org/10.1111/mmi.12800>.
 44. Mika JT, van den Bogaart G, Veenhoff L, Krasnikov V, Poolman B. 2010. Molecular sieving properties of the cytoplasm of *Escherichia coli* and consequences of osmotic stress. *Mol Microbiol* 77:200–207. <https://doi.org/10.1111/j.1365-2958.2010.07201.x>.
 45. Delpire E, Duchêne C, Goessens G, Gilles R. 1985. Effects of osmotic shocks on the ultrastructure of different tissues and cell types. *Exp Cell Res* 160:106–116. [https://doi.org/10.1016/0014-4827\(85\)90240-X](https://doi.org/10.1016/0014-4827(85)90240-X).
 46. Finan JD, Leddy HA, Guilak F. 2011. Osmotic stress alters chromatin condensation and nucleocytoplasmic transport. *Biochem Biophys Res Commun* 408:230–235. <https://doi.org/10.1016/j.bbrc.2011.03.131>.
 47. Irianto J, Swift J, Martins RP, McPhail GD, Knight MM, Discher DE, Lee DA. 2013. Osmotic challenge drives rapid and reversible chromatin condensation in chondrocytes. *Biophys J* 104:759–769. <https://doi.org/10.1016/j.bpj.2013.01.006>.
 48. Brown KE, Guest SS, Smale ST, Hahn K, Merckenschlager M, Fisher AG. 1997. Association of transcriptionally silent genes with Ikaros complexes at centromeric heterochromatin. *Cell* 91:845–854. [https://doi.org/10.1016/S0092-8674\(00\)80472-9](https://doi.org/10.1016/S0092-8674(00)80472-9).
 49. Sambrook J, W Russell D. 2001. *Molecular cloning: a laboratory manual*. Cold Spring Harbor Laboratory Press, Cold Spring Harbor, NY.
 50. Schwedock J, McCormick JR, Angert ER, Nodwell JR, Losick R. 1997. Assembly of the cell division protein FtsZ into ladder-like structures in the aerial hyphae of *Streptomyces coelicolor*. *Mol Microbiol* 25:847–858. <https://doi.org/10.1111/j.1365-2958.1997.mmi507.x>.
 51. Sevciková B, Benada O, Kofronova O, Kormanec J. 2001. Stress-response sigma factor sigma(H) is essential for morphological differentiation of *Streptomyces coelicolor* A3(2). *Arch Microbiol* 177:98–106. <https://doi.org/10.1007/s00203-001-0367-1>.
 52. Lee EC, Yu D, Martinez de Velasco J, Tessarollo L, Swing DA, Court DL, Jenkins NA, Copeland NG. 2001. A highly efficient *Escherichia coli*-based chromosome engineering system adapted for recombinogenic targeting and subcloning of BAC DNA. *Genomics* 73:56–65. <https://doi.org/10.1006/geno.2000.6451>.
 53. Gregory MA, Till R, Smith MCM. 2003. Integration site for *Streptomyces* phage ϕ BT1 and development of site-specific integrating vectors. *J Bacteriol* 185:5320–5323. <https://doi.org/10.1128/JB.185.17.5320-5323.2003>.

AUTHOR QUERIES

AUTHOR PLEASE ANSWER ALL QUERIES

1

AQau—Please confirm the given-names and surnames are identified properly by the colors.

■ = Given-Name, ■ = Surname

AQau—An ORCID ID was provided for at least one author during submission. Please click the name associated with the ORCID ID icon (🟩) in the byline to verify that the link is working and that it links to the correct author.

AQaff—Please confirm the following full affiliations or correct here as necessary. This is what will appear in the online HTML version:

^aDepartment of Biology, Lund University, Lund, Sweden

^bSwansea University Medical School, Swansea, United Kingdom

AQaff—This affiliation line will appear in the PDF version of the article and matches that on page 1 of the proof; corrections to this affiliation line may be made here **or** on page 1 of the proof:

Department of Biology, Lund University, Lund, Sweden^a; Swansea University Medical School, Swansea, United Kingdom^b

AQfund—The Funding Information below includes information that you provided on the submission form when you submitted the manuscript. This funding data will not appear in the manuscript, but it will be provided to CrossRef in order to make the data publicly available. Therefore, please check it carefully for accuracy and mark any necessary corrections. Statements acknowledging financial support may also appear within the manuscript itself (in Acknowledgments); any such statements should also be checked for accuracy, but will have no bearing on funding data deposited with CrossRef.

Funder	Grant(s)	Author(s)	Funder ID
The Swedish Research Council	621-2209-5475	Nora Ausmees	
The Crafoord Foundation	20140793	Nora Ausmees	
The Carl Trygger Foundation	CTS12:33	Nora Ausmees	

AQA—To ensure sequential order, references have been renumbered in text and in References.

Please check and correct the renumbering if necessary. If any reference should be deleted from the References list, please mark “Reference deleted” in the margin next to that entry; do not renumber subsequent references.

AQB—In Table 1, please indicate the meaning of the less than/greater than signs together and also define “Apra” in the footnote (resistance to some drug?).

AUTHOR QUERIES

AUTHOR PLEASE ANSWER ALL QUERIES

2

AQC—Please indicate in Fig. 1 what the two boxes are refer to.
